Technical University of Denmark

DTU

Analysis of Crystallographic Textures in Aluminum Plates Processed by Equal Channel Angular Extrusion

Li, Saiyi; Mishin, Oleg

DTU Library
Technical Information Center of Denmark

Analysis of Crystallographic Textures in Aluminum Plates Processed by Equal Channel Angular Extrusion

SAIYI LI[1,*] and OLEG V. MISHIN[2]

[1] School of Materials Science and Engineering, Key Laboratory of Nonferrous Metal Materials Science and Engineering of the Ministry of Education, Central South University, Changsha 410083, P. R. China

[2] Danish-Chinese Center for Nanometals, Section for Materials Science and Advanced Characterization, Department of Wind Energy, Technical University of Denmark, Risø Campus, 4000 Roskilde, Demark

Abstract

A modeling and experimental investigation has been conducted to explore the effect of processing route on texture evolution during equal channel angular extrusion (ECAE) of aluminum plate samples. It is found that although the textures in the plates develop along orientation fibers previously identified for ECAE-processed rods and bars, the main components and strength of these textures vary significantly with processing route, which may lead to considerable differences in the plastic anisotropy of the plates.

* Corresponding author

Tel: +86-731-88876621; Fax: +86-731-88876692; E-mail: saiyi@csu.edu.cn

Equal channel angular extrusion (ECAE) has been shown to be an efficient technique for producing sub-microcrystalline and nanostructured materials.[1] While the effect of processing route on the microstructure and texture development in ECAE-deformed rods and bars has been investigated in a large number of publications [2-6], only a few studies have been carried out for establishing this effect for ECAE-processed plates, for which new routes, different from those proposed for rod or bar samples, can be utilized.[7-11]

In a recent work on AA1050 plates deformed by 8 ECAE passes either without rotation between passes (route A) or with 90 deg sequential rotations about the plate normal ND (route $B_{C\langle ND\rangle}$),[11] it was found that the microstructure obtained *via* route $B_{C\langle ND\rangle}$ was more refined than that obtained *via* route A. The extent of refinement in these plates was nevertheless less significant than that in a rod sample extruded with 90 deg inter-pass rotations about the extrusion direction, ED (route $B_{C\langle ED\rangle}$).[11] The effect of the processing route on texture evolution in ECAE plates was investigated by Ferrasse *et al.*[9,10] However, these authors considered a large number of orientation fibers differing from the shear-type fibers commonly adopted for characterizing ECAE textures,[2-6] which complicates a comparison of textures in their plate samples with those in rod samples described in many other publications. To better compare the general tendencies of texture evolution during ECAE of plates with those of rod samples, a modeling and experimental investigation of textures formed by ECAE has therefore been carried out and is described in the present work for commercial purity aluminum.

A recrystallized AA1050 plate with an average grain size of ~50 μm and a pronounced cube texture was used as a starting material. Samples with dimensions of $15 \times 75 \times 75$ mm^3 were subjected to 8 ECAE passes either *via* route A or route $B_{C\langle ND\rangle}$, at room temperature, using a 90 deg die with a sharp outer corner and a sliding floor, and using an anti-seize lubricant.[11] Since during ECAE the rectangular cuboid shape of the initial sample was

distorted by shear, the leading end of the route $B_{C\langle ND\rangle}$ sample had to be trimmed after the first pass in order to reinsert the 90 deg-rotated sample into the die. For the subsequent passes *via* route $B_{C\langle ND\rangle}$, the end was only slightly ground between passes. To enable a direct comparison with these plate samples, a rod sample with a dimension of $15 \times 15 \times 75$ mm^3, prepared from the same initial material, was subjected to 8 passes *via* route $B_{C\langle ED\rangle}$.[11] Textures were measured using electron backscatter diffraction (EBSD) in the central part of the samples, covering several regions in the ED–ND section with a total area of 3~4 mm^2 for each sample. For each sample, an orientation distribution function (ODF) was derived from the EBSD-measured orientations assuming a Gaussian distribution of the type $\exp\left(\psi/\psi_0\right)^2$ with a half width of 10 deg for each measured orientation.[12,13] The series expansion method with $L_{\max} = 22$ was used for the ODF calculations.

Crystal plasticity simulations of multi-pass ECAE were carried out for each of the three routes using the Taylor model,[14] assuming ideal simple shear deformation in each pass. The initial texture in the simulations was represented by 3000 orientations, obtained from the ODF for the starting material, using the discretization method of Tóth and Van Houtte.[12,15] The deformation was accommodated by $\{111\}\langle 110\rangle$ slip. The shear rate $\dot{\gamma}^s$ and resolved shear stress τ^s of a slip system *s* were considered to obey a power-law relationship of $\dot{\gamma}^s = \dot{\gamma}_0^s \operatorname{sgn}(\tau^s)\left|\tau^s/\tau_0^s\right|^{1/m}$, where *m* is the strain-rate sensitivity index ($m = 0.02$), and $\dot{\gamma}_0^s$ and τ_0^s are respectively the reference shear rate and shear stress, which were assumed to be identical for all slip systems and did not change during deformation. ODFs were calculated from the simulated orientation set using the same procedure as for the experimentally measured orientations. As an indicator of the texture strength, a texture index[13] was calculated from the ODF of each simulated or experimental texture. For the initial texture the texture index was ~7.

Figure 1 shows the {111} pole figures for the simulated textures after 1, 2, 4 and 8 ECAE passes (N) *via* the three routes based on simple shear for each pass, together with the experimental textures after 8 passes. It is seen that the simulated texture after the first pass (Figure 1(a)) is dominated by a rotated cube component with considerable spread about the direction perpendicular to the die intersection plane. Shear-type textures become evident after the second pass (Figure 1(b)) and are observed to evolve very differently for each of the different routes. As expected from the simple shear deformation in each pass, the texture of the route A sample shows monoclinic symmetry, with the transverse direction (TD) as a dyad axis. This symmetry is partly destroyed in the $B_{C\langle ND \rangle}$ and $B_{C\langle ED \rangle}$ samples due to the additional inter-pass rotation of the samples about axes that are perpendicular to the dyad axis. The texture strength increases significantly with increasing N for route $B_{C\langle ND \rangle}$, whereas the strengthening of texture for route $B_{C\langle ED \rangle}$ is less pronounced. In contrast, no significant variation in the texture strength is found for route A (Figures 1(a-d)).

Comparison of the experimental and simulated textures after 8 passes (Figures 1(d) and (f)) reveals a good overall qualitative agreement, although the simulations somewhat overestimate the texture strength, as often found in Taylor-type texture simulations where grain interactions are neglected. The much higher texture index in Figure 1(d) for the simulated route $B_{C\langle ND \rangle}$ data as compared to the experimental result could, however, also be attributed to the fact that the trimming of the sample after the first pass was not taken into account in the simulation of this texture. This may be significant because in subsequent ECAE with a trimmed sample, plane strain compression (PSC) occurs with contraction along the pressing direction and extension along the TD in the inlet channel before its passage through the die corner. It is pertinent to mention that a similar PSC-type deformation would still occur for $N > 1$ passes *via* route $B_{C\langle ND \rangle}$ if the length of an initial plate is made shorter than its width to avoid the need to trim the sample after the first pass.

To roughly evaluate the effect of additional PSC on the texture development *via* route $B_{C\langle ND\rangle}$, the 8-pass texture for this route was simulated with additional 10 pct PSC deformation (with compression along the pressing direction) before simple shear for each of the $N > 1$ passes. The result is shown in Figure 1(e). It is apparent that this additional PSC weakens the resulting texture, leading to a better agreement between the experimental and simulated textures for the route $B_{C\langle ND\rangle}$ sample. This observation highlights the importance of considering the detailed deformation geometry in such simulations.

Figure 2 shows ODFs calculated from the EBSD data for each of the 8-pass ECAE samples. Note that the monoclinic symmetry apparent in Figure 1(f) was applied for calculation of the ODF for the route *A* sample. The locations of ideal orientation fibers (f1, f2, f3) and some key ideal orientations along them, namely, $A_{1\theta}^{*}$ $(111)[\bar{1}\,\bar{1}2]_{\theta}$, $A_{2\theta}^{*}$ $(111)[11\bar{2}]_{\theta}$, A_{θ} $(1\bar{1}1)[110]_{\theta}$, $\bar{A}_{\theta}$ $(\bar{1}1\bar{1})[\bar{1}\,\bar{1}0]_{\theta}$, B_{θ} $(1\bar{1}2)[110]_{\theta}$, $\bar{B}_{\theta}$ $(\bar{1}1\bar{2})[\bar{1}\,\bar{1}0]_{\theta}$ and C_{θ} $\{001\}\langle110\rangle_{\theta}$, all of which have previously been identified for single-pass ECAE of face-centered cubic materials in rod and bar samples,[16] are indicated in these plots. Here the Miller indices $\{hkl\}\langle uvw\rangle_{\theta}$ denote orientations that have $\{hkl\}$ planes and $\langle uvw\rangle$ directions parallel respectively to the macroscopic shear plane (MSP) and macroscopic shear direction (MSD). The f1 fiber contains only $\{111\}\langle uvw\rangle_{\theta}$ orientations, whereas the f2 and f3 fibers consist of both $\{111\}\langle uvw\rangle_{\theta}$ and $\{hkl\}\langle110\rangle_{\theta}$ orientations.

It is evident from Figure 2 that the main components in the experimental textures develop along the f1, f2 and f3 fibers. This suggests that the general tendency of texture evolution in ECAE, where the slip planes and slip directions tend to be parallel to the MSP and MSD, respectively, is valid not only for the routes investigated previously for rod and bar samples, such as routes *A* and $B_{C\langle ED\rangle}$, but also for route $B_{C\langle ND\rangle}$, which is unique to plates. The differences between these textures are mainly in the completeness of the orientation fibers and in the intensity of the main components along them. Orientation densities along

the f1, f2 and f3 fibers in the route *A* sample are relatively uniform, with the maximum

intensity near the B_θ and $\bar{B}_\theta$ components (Figure 2(a)). The other two routes lead to less

complete orientation fibers, with the maximum intensity either being intermediate between

the $A_{1\theta}^*$ and A_θ components for the route $B_{C\langle ND\rangle}$ sample (Figure 2(b)) or near $A_{1\theta}^*$ for

route $B_{C\langle ED\rangle}$ (Figure 2(c)). Overall, the textures observed in the 8-pass AA1050 samples

processed *via* routes *A* and $B_{C\langle ED\rangle}$ are similar to, though slightly weaker than, those found in

Cu rods deformed to similar strain levels.[3,5,6]

It is interesting also to compare the textures obtained in our work with previous results

on ECAE-processed plates.[9] While the experimental observations of texture strengths in the

AA1050 plates are similar to those reported by Ferrasse *et al.*[9] on Al–0.5 wt pct Cu plates,

there is a large difference in the simulation data, where the simulated textures reported in

Reference 9 are much stronger than those in our simulations. For example, for route $B_{C\langle ND\rangle}$

(termed route *D* in Reference 9) the texture indices from their Taylor simulations[9] are

almost an order of magnitude greater than those obtained in our work (see Figures 1(a-c)).

The reason for such a large discrepancy between the simulation data is unclear.

Understanding the effect of processing route on the texture evolution is of interest in

controlling the texture-induced plastic anisotropy, which is of particular significance for

ECAE-processed plates as they can be subjected to additional sheet forming processes. As a

preliminary assessment of such effects for the plate samples, the *R*-values (*i.e.*, Lankford

coefficients) of the 8-pass samples were calculated based on the experimental textures by

simulating uniaxial tensile deformation along different directions in the ED–TD plane, using

the Taylor model. The resulting values (Figure 3) suggest that the different textures in the

plate samples for different routes may lead to significantly different degrees of plastic

anisotropy. In particular, as follows from the average *R*-value (R_{ave}) and the difference

between the maximum and minimum *R*-values (R_{diff}), which measure the normal and planar

anisotropy, respectively, the route $B_{C\langle ND \rangle}$ sample is characterized by a slightly higher normal anisotropy and a much lower planar anisotropy than the route A sample. Thus, plates produced *via* route $B_{C\langle ND \rangle}$ are expected to be more suitable than plates extruded *via* route A for deep drawing applications where high normal anisotropy and low planar anisotropy are desired.

In summary, the crystal plasticity simulations reveal a strong effect of the processing route on the texture evolution during ECAE for both plate and rod samples. Such effects are verified based on EBSD measurements after 8 ECAE passes. It is shown that the textures in the plate samples develop close to shear-type orientation fibers previously identified for ECAE-processed rod and bar samples. The main components and strength of the texture developed *via* route $B_{C\langle ND \rangle}$, which is unique to plates, however, differ from those produced *via* routes A and $B_{C\langle ED \rangle}$. The differences in the textures are expected to induce considerable differences in the plastic anisotropy. Furthermore, it is shown that inclusion of an additional PSC component, corresponding to the effect of trimming the route $B_{C\langle ND \rangle}$ sample after the first ECAE pass, significantly modifies the texture predictions.

REFERENCES

1. R.Z. Valiev and T.G. Langdon: *Progr. Mater. Sci.*, 2006, vol. 51, pp. 881-981.

2. I.J. Beyerlein and L.S. Tóth: *Progr. Mater. Sci.*, 2009, vol. 54, pp. 427-510.

3. S. Li, I.J. Beyerlein, D.J. Alexander, and S.C. Vogel: *Acta Mater.*, 2005, vol. 53, pp. 2111-25.

4. S. Suwas, R. Arruffat-Massion, L.S. Tóth, J.J. Fundenberger, A. Eberhardt, and W. Skrotzki: *Metall. Mater. Trans. A*, 2006, vol. 37A, pp. 739-53.

5. S. Li, I.J. Beyerlein, and D.J. Alexander: *Mater. Sci. Eng. A*, 2006, vol. 431, pp. 339-45.

6. X. Molodova, G. Gottstein, M. Winning, and R.J. Hellmig: *Mater. Sci. Eng. A*, 2007, vols. 460-461, pp. 203-13.

7. V.M. Segal: *Mater. Sci. Eng. A*, 2008, vol. 476, pp. 178-85.

8. M. Kamachi, M. Furukawa, Z. Horita, and T.G. Langdon: *Mater. Sci. Eng. A*, 2003, vol. 361, pp. 258-66.

9. S. Ferrasse, V.M. Segal, S.R. Kalidindi, and F. Alford: *Mater. Sci. Eng. A*, 2004, vol. 368, pp. 28-40.

10. S. Ferrasse, V.M. Segal, and F. Alford: *Mater. Sci. Eng. A*, 2004, vol. 372, pp. 44-55.

11. O.V. Mishin, V.M. Segal, and S. Ferrasse: *Metall. Mater. Trans. A*, 2012, vol. 43A, pp. 4767-76.

12. P. Van Houtte: The "MTM-FHM" Software System, Katholieke Universiteit Leuven, Belgium, 2000.

13. H.J. Bunge: *Texture Analysis in Materials Science*, Butterworth, London, 1982, pp. 88-90 and 180-83.

14. G.I. Taylor: *J. Inst. Metals*, 1938, vol. 62, pp. 307-24.

15. L.S. Tóth and P. Van Houtte: *Texture Microstruct.*, 1992, vol. 19, pp. 229-44.

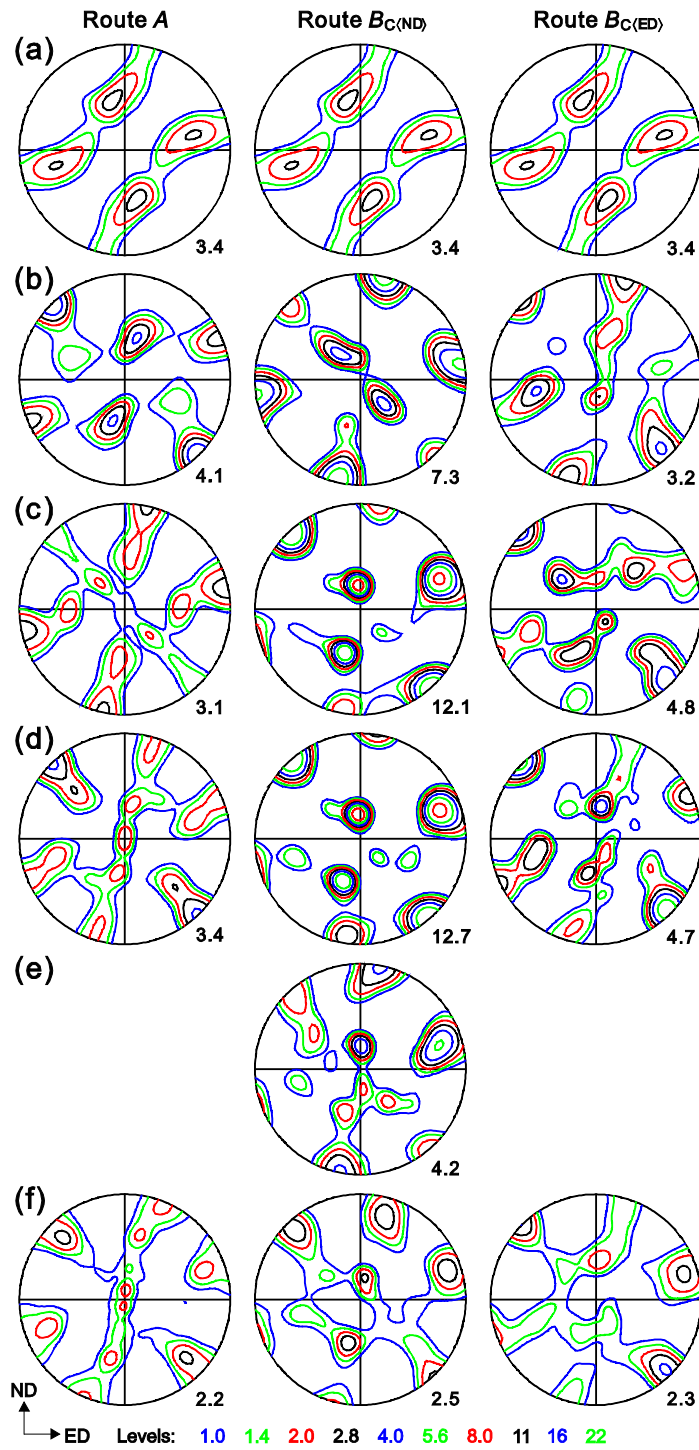16. S. Li, I.J. Beyerlein, M.A.M. Bourke: *Mater. Sci. Eng. A*, 2005, vol. 394, pp. 66-77.

Figure 1. {111} pole figures representing textures after ECAE: (*a-d*) simulated textures after 1 (*a*), 2 (*b*), 4 (*c*) and 8 (*d*) passes *via* different routes, assuming simple shear in each pass; (*e*) simulated texture after 8 passes *via* route $B_{C\langle ND\rangle}$, with PSC introduced before simple shear to mimic the effect of trimming of the sample; (*f*) experimental textures after 8 passes *via* different routes. The texture index is indicated next to each pole figure.
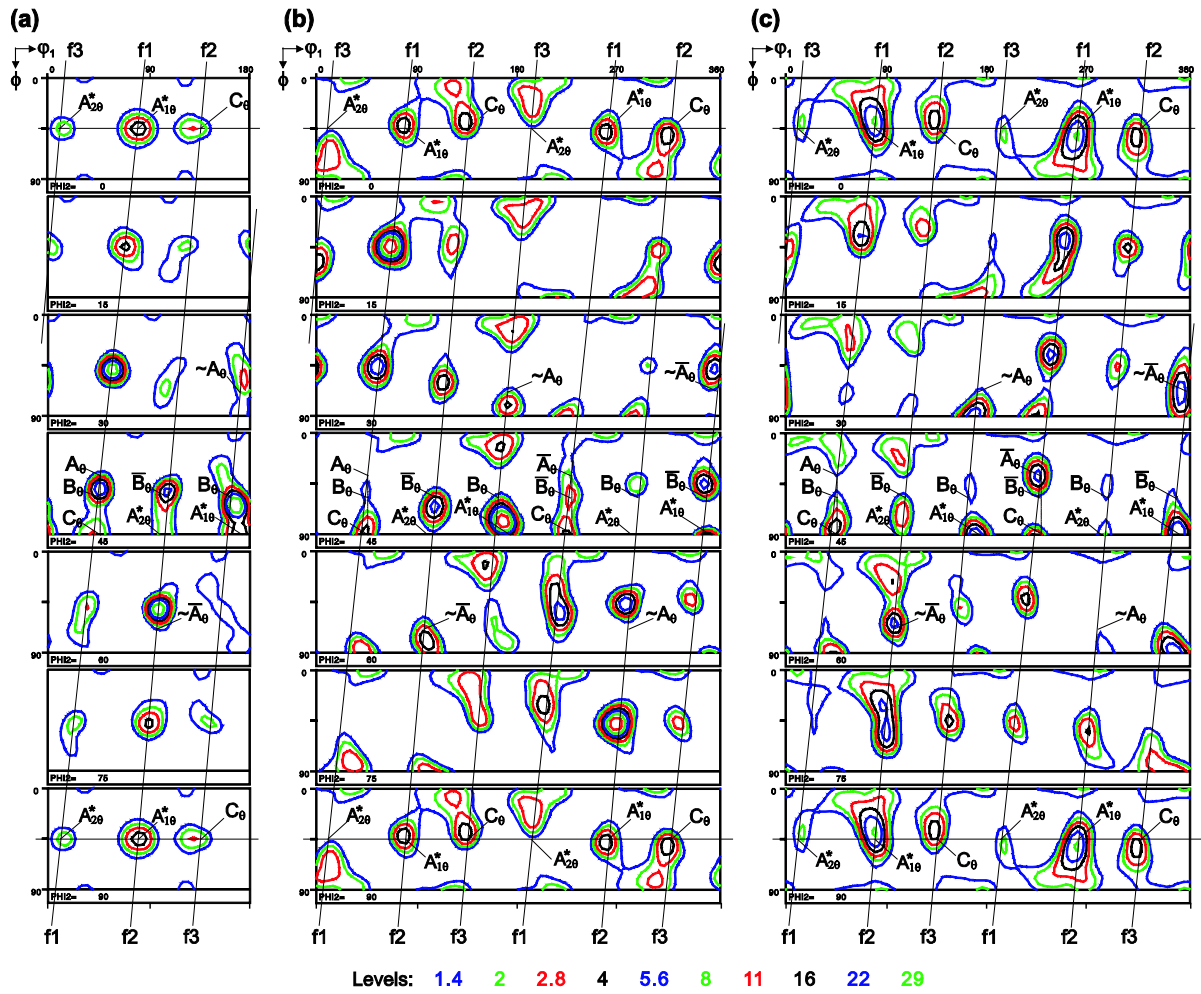
Figure 2. φ_2 = constant sections of ODFs (with Euler angles in Bunge's notation) showing experimental textures after 8 passes: (*a*) route *A*; (*b*) route $B_{C\langle ND \rangle}$; (*c*) route $B_{C\langle ED \rangle}$.
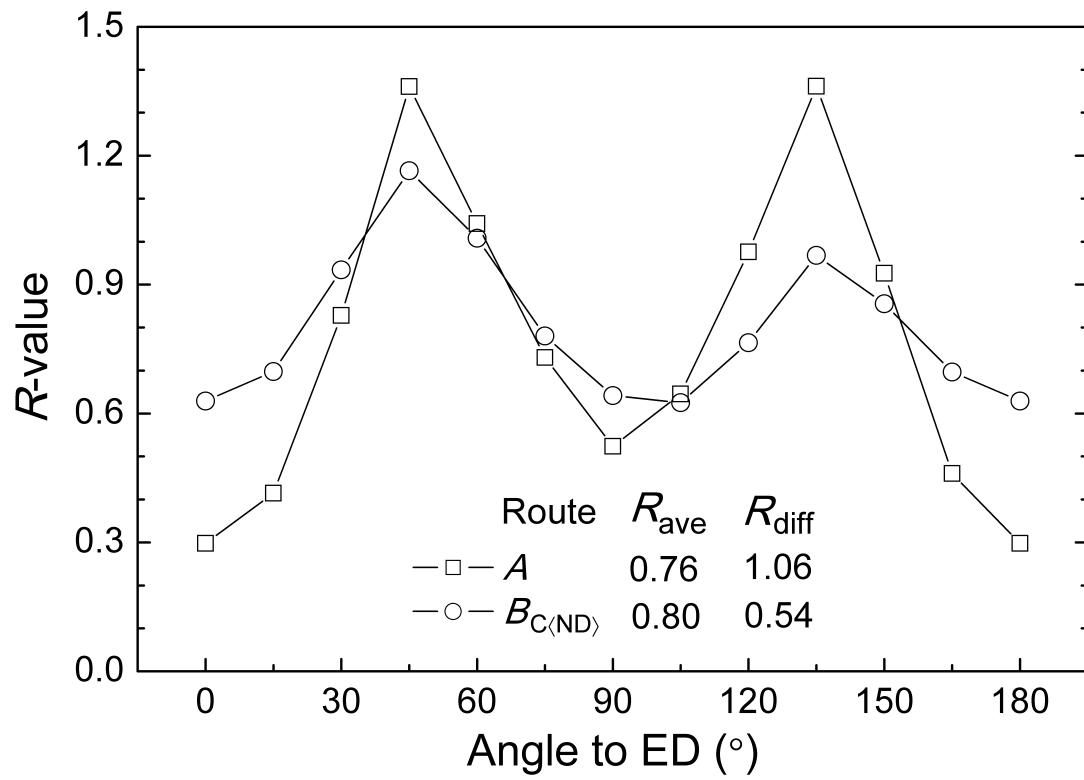
Figure 3. Predicted R-values for the plate samples after 8 passes *via* either route A or route $B_{C\langle ND\rangle}$.